Spontaneous formation of urea from carbon dioxide and ammonia in aqueous droplets

Mercede Azizbaig Mohajer[1,†], Pallab Basuri[1,†], Andrei Evdokimov[2], Grégory David[1], Daniel Zindel[1], Evangelos Miliordos[2], Ruth Signorell[1*]

[1] Department of Chemistry and Applied Biosciences, Laboratory of Physical Chemistry, ETH Zurich; Vladimir-Prelog-Weg 2, 8093 Zurich, Switzerland

[2] Department of Chemistry and Biochemistry, Auburn University; 179 Chemistry Building, Auburn, AL, USA

ABSTRACT

Urea is a key molecule in the search for the origin of life and a basic chemical produced in large quantities by industry. Its formation from ammonia and carbon dioxide requires either high pressures and temperatures or, under milder conditions, catalysts or additional reagents. Here we report the spontaneous formation of urea under ambient conditions from ammonia and carbon dioxide in the surface layer of aqueous droplets. Single optically-trapped droplets were probed using Raman bands as markers. We found the surface layer to act like a microscopic flow reactor with chemical gradients providing access to unconventional reaction pathways. This reveals a general mechanistic scheme for unique droplet chemistry. Interfacial chemistry is a possible non-energetic route for urea formation under prebiotic conditions.

[†]These authors contributed equally to this work

[*] Corresponding author. Email: rsignorell@ethz.ch (RS)

I. Introduction

Urea plays a key role in the amino acid metabolisms of mammals and amphibians via the urea cycle through which toxic ammonia is removed from the body.[1,2] It is one of the most important industrial chemicals, used primarily in the fertilizer industry, but also in many other applications, from the production of resins and explosives to medical purposes and road de-icing.[3] Urea is also relevant to astrobiology and is considered a fundamental building block for the formation of biological molecules in connection with the question of the origin of life,[4–6] e.g. as reactant in the prebiotic synthesis of cytosine and uracil and in prebiotic phosphorylation reactions. Both endogenous formation and exogenous delivery of urea have been proposed for the Early Earth ([4,5,7–10] and refs. therein).

In 1829, Friedrich Wöhler showed that urea – a byproduct of life – could be synthesized from exclusively inorganic materials,[11] thereby refuting the theory of vitalism. Today, the industrial process synthesizes urea (NH_2CONH_2) from ammonia (NH_3) and carbon dioxide (CO_2) in an overall exothermic reaction. The first step is the strongly exothermic formation of ammonium carbamate (NH_2COONH_4), which decomposes into urea and water (H_2O) in the endothermic second step. Le Chatelier's principle thus imposes contradictory requirements for shifting the equilibria towards urea, the first step being favoured by low temperature and high pressure and the second by high temperature and low pressure. The industrial process finds a compromise at high pressure (12.5-25.0 MPa) and high temperature (170-220 °C).[3] The high energy consumption and the harsh conditions of this process have prompted the search for alternative approaches that utilize catalytic pathways for urea formation ([12–19] and refs. therein).

Here, we report an intriguing pathway for urea formation that has not been previously reported: The spontaneous formation of urea in aqueous ammonia (NH_3(aq)) droplets in the presence of CO_2 gas under ambient conditions and without catalyst or additional reactants. In bulk reactions, urea formation from NH_3 and CO_2 under ambient conditions is hindered by the endothermicity of the decomposition of ammonium carbamate into urea and water. In the droplet mechanism we propose, distinct chemical gradients across the surface layer of the droplet provide access to an unconventional proton-catalysed reaction pathway in which neutral carbamic acid (NH_2COOH) replaces carbamate (NH_2COO^-) as the key intermediate. The gradients that build up across the droplet surface enable the reaction of neutral carbamic acid - which requires acidic conditions - with NH_3 - which is favoured by basic conditions. The uniqueness of droplets as chemical reactors, their potential use to scale up synthesis, and their relevance to atmospheric processes and the formation of biomolecules in the prebiotic area have attracted considerable attention in recent years ([6,18,20–40] and refs. therein). For example, conversion reactions of CO_2 into small organic molecules have been reported in microdroplets, while corresponding bulk reactions are either much slower or not observed at all.[18,36–38] Notably, the formation of protonated and deprotonated carbamic acids in CO_2-amine microdroplet reactions was proposed to originate from the superacid/superbase properties of the aqueous droplet surface.[38] The key role of the droplet pH has often been highlighted in the context of unique droplet chemistry, raising the question about stable internal pH gradients and intrinsic differences compared with pHs of bulk system – a topic that is hotly debated due to contradictory experimental results ([39,40] and refs. therein). Due to the complexity of aerosolized

droplet ensembles, it is generally challenging to provide reliable explanations for the origins and mechanisms of unusual and accelerated chemistry in these systems.

II Methods

To reduce uncertainties associated with droplet ensemble studies, we probed urea formation directly in single, optically-trapped aerosol droplets using in-situ single-droplet Raman spectroscopy (Fig. 1A and supplemental information (SI) section S1, [41,42]). With radii of only a few micrometers and femtolitre volumes, the droplets investigated here have a thousandfold higher surface to volume ratio than microdroplets of a few ten micrometers, and hence a significantly increased sensitivity to surface phenomena and product formation. The immobilization of a single droplet in a gaseous environment enables rapid (> 1 s) Raman detection over longer periods of time (many hours), precise determination of the droplet size, and control of the surrounding gas phase. Isolation of a single droplet in the gas phase combined with in-situ detection reduces potential issues with contamination and side reactions, e.g. catalytic processes at container walls. A caveat is the limited number of applicable in-situ characterization methods. Standard analytical methods are not sensitive enough. We thus supplemented the single droplet studies with droplet ensemble experiments (section S2) using ex-situ characterization with gas chromatography–mass spectrometry (GC-MS) and carbon-13 NMR (^{13}C NMR) after sample collection. Based on the evidence for spontaneous urea formation gained from the experimental results, we propose a mechanism, highlighting the unique role of the droplet surface.

III Results and Discussion

III.1 Reaction in single droplets

Figure 1B shows Raman spectra of a single, aqueous ammonia solution (NH_3(aq)) droplet before (t < 0 min, light grey) and after (t > 0 min, medium and dark grey) exposure to humidified CO_2 gas (0.5 – 1 bar) in the region of the strong C-N stretching vibration of urea (max. ~1003 cm^{-1}).[43] No signal is detected prior to CO_2 exposure. After CO_2 exposure, a Raman band around 1008 cm^{-1} appears, increasing in intensity within the first ~30 minutes (t = 30 min). Reference spectra for aqueous droplets containing pure compounds with Raman bands in this range (urea, bicarbonate (HCO_3^-), and carbamate; Fig. S4) reveal that this band can be decomposed into two components, one arising from urea (Fig. 1C, red area) and the other from bicarbonate (blue area, max.~1013 cm^{-1}). Clearly, urea has spontaneously formed under the unique conditions in droplets. Different single droplet studies reveal an average urea concentration of 42 ± 10 mM when the reaction has gone to completion (sections S4, S6). Inferred bicarbonate concentrations together with the absence of significant amounts of carbamate (max. ~1037 cm^{-1}) and carbonate (CO_3^{2-}, max. ~1065 cm^{-1}) place the average droplet pH at ~6.7 for reaction times beyond ~18 min (assuming equilibrium; section S5). By varying the intensity of the trapping laser, we verified that urea formation is neither photoinduced nor thermally induced.

The essential components for the formation of urea in droplets are NH_3 and CO_2. If CO_2 is replaced by nitrogen (N_2) gas under otherwise identical conditions, no urea is formed (Fig. 1D). The same holds in the absence of dissolved ammonia in the droplet (Fig. 1E). In contrast to Fig. 1B, no bicarbonate is observed in Fig. 1E because at the resulting pH of ~4 the equilibrium concentration of bicarbonate lies below the detection limit of the droplet Raman spectra (~10 mM). Droplets containing ammonium salts do not form detectable amounts of urea either, as shown for aqueous ammonium carbonate and ammonium carbamate droplets in CO_2 gas (Figs. 1F and 1G, respectively). The salt spectra in Figs. 1F and G contain similar contributions from bicarbonate (blue) and carbamate (grey), consistent with an equilibrium droplet pH of ~7.6 (section S5). The corresponding bicarbonate concentration of 650 mM puts the limit for urea detection by band deconvolution at ~20 mM. Given that the NH_4^+ concentration is about ten times larger than in Fig. 1C, the observation that urea is not formed in much larger amounts in the ammonium salt droplets indicates that the unexpected formation of urea in Figs. 1B and C relies on the presence of unprotonated NH_3.

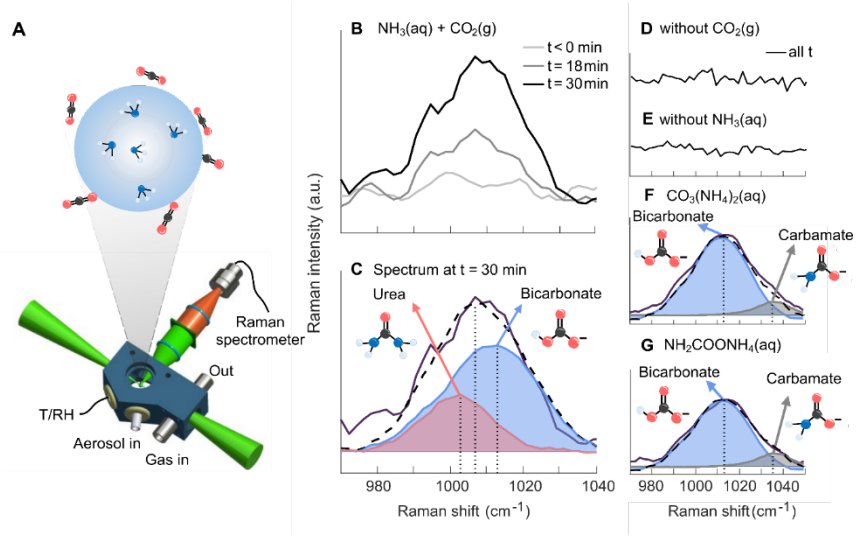

Figure 1. (A) Top: Schematic representation of a single droplet with ammonia and carbon dioxide molecules at the surface. Bottom: Trapping cell (blue) for immobilization of a single droplet by counter-propagating optical tweezers (green cones). (B) Single-droplet Raman spectra recorded before ($t < 0$ min) and after ($t > 0$ min) exposure of an aqueous ammonia (NH_3(aq)) droplet (radius 2 µm) to CO_2(g) gas. (C) The decomposition of the Raman spectrum at $t = 30$ min (full black line) shows that urea (red, 33mM) is formed in addition to bicarbonate (blue, 83 mM). The dashed black line is the sum spectrum of urea and bicarbonate. The vertical dotted lines indicated the positions of the band maxima of urea (1003 cm^{-1}), the sum spectrum (1008 cm^{-1}), and the bicarbonate (1013 cm^{-1}). (D) Single droplet spectrum of an NH_3(aq) droplet in nitrogen gas (N_2), i.e. without the addition of CO_2 gas. (E) Single droplet spectrum of a water droplet (i.e. without NH_3) in CO_2 gas. No Raman bands and thus no urea formation was seen for D and E. (F) Single droplet spectrum of a 1M ammonium carbonate droplet in in CO_2 gas. (G) Single droplet spectrum of a 1M ammonium carbamate droplet in in CO_2(g). F and G do not show detectable amounts of urea. The decomposition of the Raman spectra (full black lines) shows that bicarbonate (blue, max. 1013 cm^{-1}) and carbamate (grey, 1037 cm^{-1}) are formed in addition to bicarbonate (blue). The dashed black lines are the sum spectra. The vertical dotted lines indicated the positions of the band maxima of bicarbonate (1013 cm^{-1}), the sum spectrum (1013 cm^{-1}), and carbamate (1037 cm^{-1}).

III.2 Reaction in droplet ensembles and in bulk liquid

In complementary droplet ensemble experiments (Fig. 2A, sections S2, S8), an aqueous ammonia solution was sprayed into a round-bottom flask filled with humidified CO_2 gas (1 bar) and a small amount of liquid water at the bottom. After deposition of the droplets, the liquid at the bottom was analysed with GC-MS, ^{13}C NMR and Raman spectroscopy. The maximum reaction time in the droplet phase was limited by the short residence time of the droplets in the gas phase (< 3 min), yielding only very minor amounts of urea per droplet compared with the single droplet experiment (Fig. 1C). GC-MS indeed confirmed the formation of urea (Fig. 2C). Very weak signals of urea could also be identified by ^{13}C NMR at chemical shifts of ~162.8 ppm (Fig. 2B). The Raman spectrum shows the presence of bicarbonate (blue) and carbamate (grey) (Fig. 2D), but lacks the sensitivity to detect urea in such small concentrations. While the GC-MS and ^{13}C NMR do confirm urea formation, droplet ensemble measurements alone would have been insufficient to confirm formation in the droplet phase as opposed to e.g. reactions on container surfaces. However, together with the single droplet measurements these additional data sets provide convincing evidence for urea formation from NH_3 and CO_2 in the unique environment of small droplets.

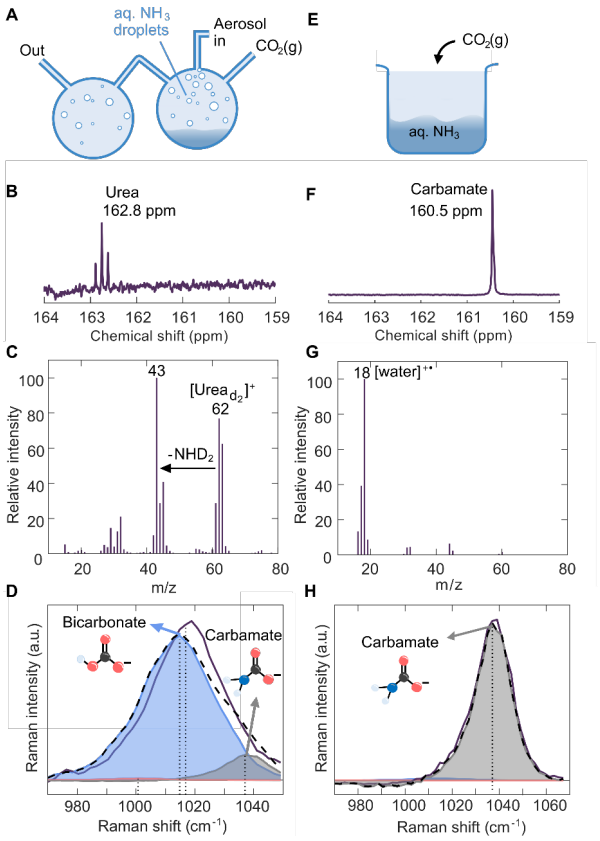

Figure 2. Droplet ensemble (A to D) and bulk experiments (E to H). (A) Schematic representation of the droplet ensemble setup. (B) The ^{13}C NMR spectrum of the droplet ensemble sample shows a weak urea signal at 162.8 ppm. (C) The mass spectrum from GC-MS of a partially deuterated droplet ensemble sample shows the characteristic patterns of partially deuterated urea (section S8). (D) The Raman spectrum of the droplet ensemble sample does not show a detectable urea band, but as in Figs. 1F and G contributions from bicarbonate (blue) and carbamate (grey). (E) Schematic representation of the setup for bulk studies. (F) The ^{13}C NMR spectrum of the bulk sample shows a carbamate signal at

160.5 ppm, but no urea. (G) The mass spectrum from GC-MS of a partially deuterated bulk sample shows the background spectrum, containing mostly water but no urea. (H) The Raman spectrum of the bulk sample shows only the carbamate band (grey), but no urea.

As is well known, this reaction does not take place in conventional liquid bulk reaction systems at ambient temperatures and pressures, as confirmed by bulk control experiments (Fig. 2E-H, Section S3). In the range of interest, ^{13}C NMR and Raman spectra only show signals from carbamate (at 160.5 ppm and max. 1037 cm^{-1}, respectively), but not from urea. The GC-MS also confirms the absence of urea in these bulk experiments.

III.3 Proposed mechanism

The confined space of droplets must have opened a new reaction pathway. What could be the mechanism? The fact that urea formation from CO_2 and NH_3 occurs exclusively in droplets (Figs. 1 B, C and Figs. 2 B-D), but not in the bulk (Figs. 2 F-H) implies that the reaction takes place near the surface, presumably in the interfacial region governed by pronounced concentration gradients. In the industrial synthesis of urea at high temperature and pressure, carbamate is the key intermediate [3]. This is clearly not the case for the formation of urea under the ambient conditions of our experiments where ammonium carbamate does not react any further, neither in the bulk (Figs. 2 F-H) nor in the droplets (Figs. 1F,G) - at least not to a measurable extent. A conceivable reaction intermediate is carbamic acid itself. Although unstable with respect to decomposition into NH_3 and CO_2, it could still play the role of the reactive intermediate in a reaction at the droplet surface under sufficiently acidic conditions.

To form urea from carbamic acid requires the addition of a second NH_3 molecule, which must be provided in unprotonated form (see above). If this originated from the droplet interior, one would expect a much more pronounced urea contribution to the ammonium salt spectra than observed in Figs. 1F and G, where the NH_3(aq) concentration is 1-2 orders of magnitude larger than in the case of Fig. 1C (section S5). Instead, we hypothesize that the addition of the second NH_3 to form urea involves the reaction with surface adsorbed, partially solvated NH_3 molecules. In the case of Figs. 1B and C, the spraying of the initially highly concentrated NH_3(aq) solution (25% w/w) into the trapping cell (Fig. 1A) loads the inner surfaces of the cell with macroscopic amounts of NH_3(aq). This provides a continuous supply of gaseous NH_3(g) in the droplet's environment. Assuming equilibrium, we estimate a NH_3(g) partial pressure of ~0.4 Pa (section S5). This ammonia gas source is missing in the ammonium salts experiments (Figs. 1F, G).

To corroborate our mechanistic hypothesis on a molecular level, we performed quantum chemical calculations for cluster models representing local conditions in an interfacial layer at the surface ([44,45], section S10). NH_3 enters the reaction as a partially solvated, surface adsorbed species, while CO_2 is present in an acidic subsurface layer. To avoid artefacts in the energetics, we kept the number of hydrogen bonds constant throughout each reaction step. The calculations confirm that the formation of neutral carbamic acid in an acidic aqueous environment is both thermodynamically and kinetically favourable (Fig. 3 steps A→→D, [19]). The critical steps for the formation of urea are the addition of the second ammonia (step D→E) and the subsequent elimination of H_2O (step E→F, [19]). In contrast to carbamic acid, its conjugate base, carbamate,

does not even add NH_3 in the cluster model (section S10, models S11 and S12), consistent with the observation that urea does not form from carbamate in aqueous bulk solutions under ambient conditions (Fig. 2F-H). Additional cluster calculations also indicate that the formation of urea from carbamic acid is specifically catalysed by H_3O^+(e.g. not by NH_4^+; section S10, models S9 and S10), implying the requirement of an at least locally low pH. This would be consistent with the idea of a substantially reduced surface pH (<6.7) compared with the average droplet pH. Overall, the mechanism consists of the proton-catalysed formation of neutral carbamic acid which continues to react with unprotonated NH_3, again in a proton-catalysed reaction, to form urea. The mass spectroscopic observation of protonated carbamic acid formed by the reaction of CO_2 with amines in electrosprayed acetonitryl droplets in the presence of water [38] lends further support to our proposed mechanism. The addition of a second amine to form substituted urea derivatives was not observed in that study. Whether this was due to the much shorter time scale (ms) than in our experiments (min to hours) or to intrinsic kinetic or thermodynamic hindrance remains unclear.

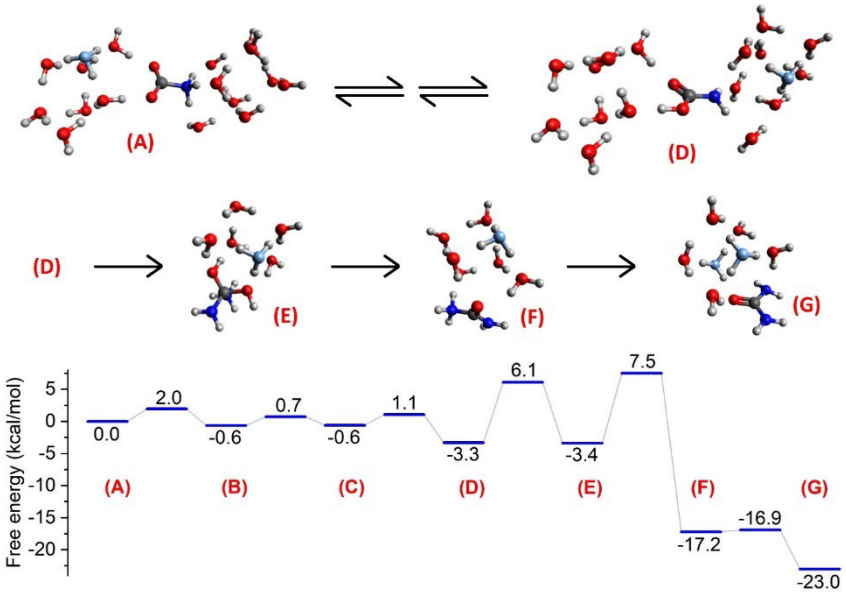

Figure 3: Structures and free energy diagram (bottom row) for the formation of urea from NH_3 and CO_2. Red/blue/grey/white balls represent O/N/C/H atoms. Light blue indicates the O atom of hydroniums. The top row describes the formation of carbamic acid as reactive intermediate through a number of fast reversible steps (A) to (D) establishing a quasi-equilibrium. The second row shows the rate determining addition of the second NH_3 to carbamic acid (see Section S10 and Fig. S15).

IV Conclusion

The spontaneous formation of urea is a prime example for droplet chemistry distinct from bulk reactions, highlighting a general mechanistic scheme unique to droplets. The high surface-to-volume ratio of a droplet gives prominence to reactions in the interfacial layer near the surface where pronounced concentration gradients establish the microscopic equivalent of a flow reactor connected by molecular transport to the reservoirs of the droplet interior on one side and the gas phase on the other (Fig. 4). In this way interfacial reaction systems can solve

the dilemma of bulk reactions hindered by mutually exclusive conditions for the coexistence of key reactants. Here it is the requirement for an acidic environment to provide neutral carbamic acid and enable proton catalysis on the one hand, and the need for unprotonated NH_3 on the other hand. The pH gradient across the interfacial layer creates the required acidic environment while a continuous supply of NH_3 is provided in the form of adsorbed partially solvated molecules. The product urea is continuously removed from the reaction area by diffusion into the droplet interior.

We anticipate that the general mechanistic scheme proposed here is of relevance to a number of unusual droplet reactions. Chemical potential gradients across the surface layer enable reactions between reactants that do not coexist in sufficient amounts under equilibrium conditions, thereby opening up alternative, unconventional reaction pathways. Such alternative pathways may have been important for the abiotic synthesis of precursor molecules, such as urea, and the subsequent formation of simple biomolecules necessary for the evolution of life, e.g. at the surfaces of aerosol droplets and particles, lakes, and oceans.[4–6]

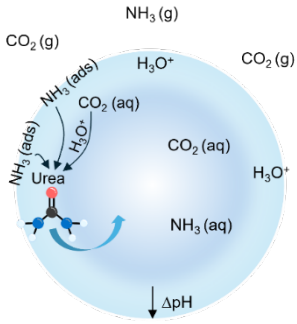

Figure 4: Urea is formed in a multistep, proton-catalyzed reaction between partially solvated, surface adsorbed ammonia (NH_3(ads)) and dissolved carbon dioxide (CO_2(aq)) in a surface layer, where a pH gradient creates the necessary acidic conditions.

Acknowledgements: We are grateful to P. Albrecht, M. Steger, J. Schürmann and the NMR and the Molecular and Biomolecular Analysis Services at ETHZ for technical support. We thank O. Reich and M. Gleichweit for discussions regarding the trapping setup. This project has received funding from the Swiss National Science Foundation (project 200020_200306) and the United States National Science Foundation (Grant No. CHE-1940456). RS acknowledges support by the Centre for Origin and Prevalence of Life (COPL) at ETHZ.

References:

1. Krebs, H. A. & Henseleit, K. Untersuchungen uber die Harnstoffbildung im Tierkörper. *Hoppe-Seyler's Z Physiol Chem* **210**, 33–66 (1932).
2. Nelson, D. L., Cox, M. M. & Lehninger, A. L. *Lehninger Principles of Biochemistry*. (W.H. Freeman and Company, ed. 6, 2013).
3. Meessen, J. H. Urea. in *Ullmann's Encyclopedia of Industrial Chemistry* (Wiley-VCH, Weinheim, 2010).
4. Horneck, G. & Baumstark-Khan, C. *Astrobiology: The Quest for the Conditions of Life*. (Springer, ed. 1, 2012).
5. Kolb, V. M. *Astrobiology an evolutionary approach*. (Taylor & Francis Group, ed. 1, 2015).
6. Rapf, R. J. & Vaida, V. Sunlight as an energetic driver in the synthesis of molecules necessary for life. *Physical Chemistry Chemical Physics* **18**, 20067–20084 (2016).
7. Brigiano, F. S., Jeanvoine, Y., Largo, A. & Spezia, R. The formation of urea in space. *A&A* **610**, (2018).
8. Potapov, A., Theulé, P., Jäger, C. & Henning, T. Evidence of Surface Catalytic Effect on Cosmic Dust Grain Analogs: The Ammonia and Carbon Dioxide Surface Reaction. *Astrophys J Lett* **878**, L20 (2019).
9. Förstel, M. *et al.* Synthesis of urea in cometary model ices and implications for Comet 67P/Churyumov–Gerasimenko. *Chemical Communications* **52**, 741–744 (2016).
10. Miller, S. L. & Urey, H. C. Organic Compound Synthesis on the Primitive Earth. *Science* **130**, 245–251 (1959).
11. Wöhler, F. Ueber künstliche Bildung des Harnstoffs. *Ann Phys* **88**, 253–256 (1828).
12. Barzagli, F., Mani, F. & Peruzzini, M. From greenhouse gas to feedstock: formation of ammonium carbamate from CO2 and NH3 in organic solvents and its catalytic conversion into urea under mild conditions. *Green Chemistry* **13**, 1267–1274 (2011).
13. Manaka, Y., Nagatsuka, Y. & Motokura, K. Organic bases catalyze the synthesis of urea from ammonium salts derived from recovered environmental ammonia. *Sci Rep* **10**, 2834 (2020).
14. Srinivas, B. *et al.* Photocatalytic Synthesis of Urea from in situ Generated Ammonia and Carbon Dioxide. *Photochem Photobiol* **88**, 233–241 (2012).
15. Zhu, X., Zhou, X., Jing, Y. & Li, Y. Electrochemical synthesis of urea on MBenes. *Nat Commun* **12**, 4080 (2021).
16. Liu, Y. *et al.* C-Bound or O-Bound Surface: Which One Boosts Electrocatalytic Urea Synthesis? *Angewandte Chemie International Edition* **62**, e202300387 (2023).
17. Chen, C. *et al.* Coupling N_2 and CO_2 in H_2O to synthesize urea under ambient conditions. *Nat Chem* **12**, 717–724 (2020).

18. Song, X. *et al.* One-step Formation of Urea from Carbon Dioxide and Nitrogen Using Water Microdroplets. *J Am Chem Soc* **145**, 25910–25916 (2023).

19. Ding, J. *et al.* Direct synthesis of urea from carbon dioxide and ammonia. *Nat Commun* **14**, 4586 (2023).

20. Kusaka, R., Nihonyanagi, S. & Tahara, T. The photochemical reaction of phenol becomes ultrafast at the air–water interface. *Nat Chem* **13**, 306–311 (2021).

21. Rossignol, S. *et al.* Atmospheric photochemistry at a fatty acid–coated air-water interface. *Science (1979)* **353**, 699–702 (2016).

22. Corral Arroyo, P. *et al.* Amplification of light within aerosol particles accelerates in-particle photochemistry. *Science (1979)* **376**, 293–296 (2022).

23. Liu, T. & Abbatt, J. P. D. Oxidation of sulfur dioxide by nitrogen dioxide accelerated at the interface of deliquesced aerosol particles. *Nat Chem* **13**, 1173–1177 (2021).

24. Rovelli, G. *et al.* A critical analysis of electrospray techniques for the determination of accelerated rates and mechanisms of chemical reactions in droplets. *Chem Sci* **11**, 13026–13043 (2020).

25. Chen, C. J. & Williams, E. R. The role of analyte concentration in accelerated reaction rates in evaporating droplets. *Chem Sci* **14**, 4704–4713 (2023).

26. Holden, D. T., Morato, N. M. & Cooks, R. G. Aqueous microdroplets enable abiotic synthesis and chain extension of unique peptide isomers from free amino acids. *Proceedings of the National Academy of Sciences* **119**, e2212642119 (2022).

27. Murke, S., Chen, W., Pezzotti, S. & Havenith, M. Tuning Acid–Base Chemistry at an Electrified Gold/Water Interface. *J Am Chem Soc* **146**, 12423–12430 (2024).

28. Mehrgardi, M. A. *et al.* Catalyst-Free Transformation of Carbon Dioxide to Small Organic Compounds in Water Microdroplets Nebulized by Different Gases. *Advanced Science* **11**, 2406785 (2024).

29. Basuri, P. *et al.* Spontaneous α-C−H Carboxylation of Ketones by Gaseous CO2 at the Air-water Interface of Aqueous Microdroplets. *Angewandte Chemie International Edition* **63**, e202403229 (2024).

30. Klijn, J. E. & Engberts, J. B. F. N. Fast reactions 'on water'. *Nature* **435**, 746–747 (2005).

31. Huang, K.-H., Wei, Z. & Cooks, R. G. Accelerated reactions of amines with carbon dioxide driven by superacid at the microdroplet interface. *Chem Sci* **12**, 2242–2250 (2021).

32. Craig, R. L. *et al.* Direct Determination of Aerosol pH: Size-Resolved Measurements of Submicrometer and Supermicrometer Aqueous Particles. *Anal Chem* **90**, 11232–11239 (2018).

33. Li, M. *et al.* Spatial homogeneity of pH in aerosol microdroplets. *Chem* **9**, 1036–1046 (2023).

34. Narayan, S. *et al.* “On Water”: Unique Reactivity of Organic Compounds in Aqueous Suspension. *Angewandte Chemie International Edition* **44**, 3275–3279 (2005).

35. Wei, Z., Li, Y., Cooks, R. G. & Yan, X. Accelerated reaction kinetics in microdroplets: Overview and recent developments. *Annu Rev Phys Chem* **71**, 31–51 (2020).

36. Banerjee, S., Gnanamani, E., Yan, X. & Zare, R. N. Can all bulk-phase reactions be accelerated in microdroplets? *Analyst* **142**, 1399–1402 (2017).

37. Wilson, K. R. & Prophet, A. M. Chemical kinetics in microdroplets. *Annu Rev Phys Chem* **75**, (2024).

38. Yan, X., Bain, R. M. & Cooks, R. G. Organic Reactions in Microdroplets: Reaction Acceleration Revealed by Mass Spectrometry. *Angewandte Chemie International Edition* **55**, 12960–12972 (2016).

39. Yan, X. Emerging microdroplet chemistry for synthesis and analysis. *Int J Mass Spectrom* **468**, 116639 (2021).

40. Song, X. & Zare, R. N. The power of microdroplet photochemistry. *Chem Sci* **15**, 3670–3672 (2024).

41. Esat, K., David, G., Poulkas, T., Shein, M. & Signorell, R. Phase transition dynamics of single optically trapped aqueous potassium carbonate particles. *Physical Chemistry Chemical Physics* **20**, 11598–11607 (2018).

42. Reid, J. P. Particle levitation and laboratory scattering. *J Quant Spectrosc Radiat Transf* **110**, 1293–1306 (2009).

43. Wen, N. & Brooker, M. H. Ammonium Carbonate, Ammonium Bicarbonate, and Ammonium Carbamate Equilibria: A Raman Study. *J Phys Chem* **99**, 359–368 (1995).

44. Ariyarathna, I. R., Pawłowski, F., Ortiz, J. V. & Miliordos, E. Aufbau Principle for Diffuse Electrons of Double-Shell Metal Ammonia Complexes: The Case of M(NH3)4@12NH3, M = Li, Be+, B2+. *J Phys Chem A* **124**, 505–512 (2020).

45. Yanai, T., Tew, D. P. & Handy, N. C. A new hybrid exchange–correlation functional using the Coulomb-attenuating method (CAM-B3LYP). *Chem Phys Lett* **393**, 51–57 (2004).